Analysis of magnetic-resonance signals from mixed lattices with application to the AsO_4^{4-} center in the $Rb_{1-x}(NH_4)_xH_2PO_4$ proton glass

A. N. Klymachyov, R. Xu, and A. Wandelt
Department of Chemistry, West Virginia University, Morgantown, West Virginia 26506

P. K. Kahol
Department of Physics, Wichita State University, Wichita, Kansas 67260

N. S. Dalal*
Department of Chemistry, West Virginia University, Morgantown, West Virginia 26506
(Received 5 September 1995)

Electron paramagnetic resonance (EPR) signals of the AsO_4^{4-} radical embedded in the ferroelectric-antiferroelectric mixed lattice $Rb_{1-x}(NH_4)_xH_2PO_4$, the so-called proton glass, exhibit unusual features: the line centers shift concomitant with an overall broadening, but not as predicted by standard motional narrowing models. Earlier studies have interpreted this phenomenon as implying a direct evidence for the existence of a ''fast'' ferroelectric-antiferroelectric exchange process. In contrast, the current work presents a phenomenological model that ascribes the observed signal to the resultant of a statistical average of hyperfine splittings over the various possible near-neighbor interactions, with little contribution from motional averaging or exchange processes. The methodology presented yields information on the range of interactions in a mixed lattice, and should be applicable to other related cases such as NMR analysis of mixed systems.

I. INTRODUCTION

This report presents a simple theoretical procedure for analyzing the line shapes of EPR signals from a spin probe that is dilutely substituted in a crystal lattice of varying composition, i.e., a homogeneous (single) crystal grown from two compounds. The mixed lattice considered here is that whose components interact differently with the spin probe so that the probe's spectra are characteristic of each component. The main impetus for this undertaking came from some recent EPR studies of the mixed lattice $Rb_{1-x}(NH_4)_xH_2PO_4$, henceforth RADP, in which the AsO_4^{4-} center was utilized as a spin probe and the reported results were not well understood.[1–6] RADP has attracted considerable attention recently because its single crystals exhibit glasslike dielectric behavior,[7,8] for example, a wide distribution of relaxation times,[7–12] and different magnitudes for field-cooled and zero-field-cooled susceptibilities,[13] for the composition range $0.21 < x < 0.74$. This system has thus been acclaimed to constitute a fundamentally new class of (spin) glass systems.[9,10,14] The glassy behavior is essentially a result of the existence of competing interactions in the RADP lattice,[7–14] since RbH_2PO_4 (RDP) is ferroelectric and $NH_4H_2PO_4$ (ADP) is antiferroelectric.[15] In a mixed crystal of RDP and ADP, therefore, a polar probe would be expected to experience competing ferroelectric and antiferroelectric interactions. Since the AsO_4^{4-} center had proven to be a sensitive probe of the slow motional dynamics and microscopic changes near the ferroelectric and antiferroelectric transitions of the RDP/ADP type crystals,[16] it was natural to examine its utility for the mixed lattice.[17] Additionally, earlier EPR studies of the AsO_4^{4-} center substituted into single crystals of RDP and ADP had demonstrated that this probe's EPR signals were distinctly different when used in the two lattices separately: a relatively sharp doublet for ADP and a broad singlet for RDP (for $H \| a + 45°$).[18,19] Subsequent measurements from RADP mixed crystals showed a systematic shift in line position as well as line shape of the individual features as a function of the composition variable x.[2–6] These changes were first interpreted to result from a fast exchange between ferroelectric and antiferroelectric configurations around the AsO_4^{4-} probe,[2] while later studies ascribed them to a compound result of strain broadening and slow motional processes,[3–5] but some controversy still exists.[6] The present analysis indicates that the dominant features of the spectra in the mixed lattice can be explained as being a result of statistical averaging together with some broadening due to slow motional processes. Moreover, the presented methodology is general enough to be applicable for other types of spectroscopic studies (for example, NMR) of mixed lattices.

Our organization of the article is as follows. The experimental apparatus and sample preparation techniques are described in the next section. An overview of the crystal structure and bonding is presented in Sec. III. The salient features of the EPR spectra from the mixed crystals are described in Sec. IV. A theoretical model that can satisfactorily explain the observed results and its comparison with the observed data are discussed in Sec. V. The concluding section summarizes the main implications of this study for the problem of proton glass and related areas.

II. EXPERIMENTAL DETAILS

Mixed crystals of $Rb_{1-x}(NH_4)_xH_2PO_4$ ($x=0.0$, $x=0.1$, $x=0.2,\ldots,x=0.9$, $x=1.0$) were grown by slow evaporation of aqueous solutions containing about 0.1 mol % $NH_4H_2AsO_4$. $NH_4H_2AsO_4$ was added in order to replace some of the PO_4^{3-} units by AsO_4^{3-} groups. The doped crys-

tals were x irradiated in order to generate the EPR-active AsO_4^{4-} center.[16] The x content of the mixed crystals was ascertained via measurements of the Rb content through EPR analysis as outlined in Sec. V. All of the crystals utilized in this study were rectangular plates with prismatic ends and their longest dimension was found to be the unique (polar) direction, the c axis. EPR measurements were made at the X-band (~9.5 GHz) frequencies utilizing a computer-controlled Bruker ER-300 EPR spectrometer. The microwave frequency was measured with a Hewlett-Packard (HP-5340A) frequency counter while the Zeeman field was calibrated using the standard free radical 1,1-diphenyl-2-picrylhydrazyl (DPPH). Crystal orientation was accomplished using a Bruker goniometer with EPR measurements made at every 5° in the three mutually perpendicular crystal planes ab, bc, and ca at every composition x. Microwave power level and magnetic field modulation amplitude were optimized to obtain maximum signal amplitude without any noticeable line shape distortion.

III. STRUCTURAL DETAILS

With the view of being able to provide a clear physical description of our theoretical model as well as for later discussion, it seems useful to give a brief overview of the structural and bonding properties of RDP, ADP, and the RADP (proton) glass system. Both RDP and ADP grow as rectangular parallel-piped crystals, exhibiting a tetragonal ($I42d$) symmetry, with the c axis as the largest dimension.[15] The structure is built from chains of PO_4^{3-} anions and Rb^+ (or NH_4^+) cations, alternating along the c axis at $c/2$ intervals. Each PO_4^{3-} anion is linked to a neighboring PO_4^{3-} unit through O-H···O hydrogen bonds essentially perpendicular to the c direction, i.e., along the crystallographic a and b directions. The H's are found to be dynamically disordered between two sites of a double-minimum potential well along the O-H···O bond.[15] On cooling below about 148 K, the H's order in one of these two sites and this process results in a (nearly) first-order structural as well as dielectric transition in both RDP and ADP. However, the H's order ferroelectrically in RDP but antiferroelectrically in ADP. Thus, when a crystal is grown as a mixture of RDP and ADP, i.e., $RDP_{1-x}ADP_x$, the proton lattice experiences competing interactions: the H's in a microscopic unit containing the Rb cation would have a tendency to align ferroelectrically, whereas those around an NH_4^+-containing subunit would experience antiferroelectric forces. Thus the H's in a mixed RDP/ADP crystal would behave as a glassy system, providing the justification for the term ''proton glass'' for RADP (7–14). It is also important to note that the mixed lattice retains its tetragonal symmetry even in the glassy phase,[20] well below 148 K.

The AsO_4^{4-} radical is generated in the RDP, ADP, and RADP crystals by a dilute (=0.1 mol %) substitution of the PO_4^{3-} moieties by AsO_4^{3-} units and then x-ray irradiation of the doped crystals to convert AsO_4^{3-} anions to AsO_4^{4-} radicals.[16] Thus the AsO_4^{4-} radical acts as a microscopic probe for sampling the environment around the PO_4^{3-} units. Detailed EPR and electron-nuclear double resonance (ENDOR) measurements of the AsO_4^{4-} radical have established that the radical retains the site symmetry of the substituted sites.[16,18,21] Furthermore, this polar radical is coupled to the lattice via strong Coulombic forces since it has been shown[22] that relatively weak electric fields can alter the polar state of the radical even at temperatures above the Curie point. Thus the EPR spectra of this center would be expected to be a sensitive probe for monitoring the nature of competing interactions in the RADP type of mixed lattices.

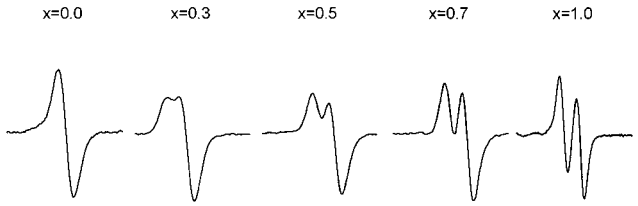

FIG. 1. Lowest-field ($m=3/2$) components of EPR spectra of the AsO_4^{4-} center in $Rb_{1-x}(NH_4)_xH_2PO_4$ for $x=0.0$, 0.3, 0.5, 0.7, and 1.0.

IV. SALIENT FEATURES OF THE EPR SPECTRA AS A FUNCTION OF COMPOSITION

We begin by summarizing the evolution of the complex line shape of the EPR signals as the composition is varied from that of pure RDP ($x=0.0$) toward pure ADP ($x=1.0$). The salient features of the observed line shape would then be used as the basis for our theoretical model presented in the following section (V).

Figure 1 shows some typical spectra for five selected compositions $x=0.0$, 0.3, 0.5, 0.7, and 1.0. The spectral feature depicted is the lowest-field ($m_I=3/2$) component of the ^{75}As hyperfine quartet for the orientation $H\|(a+45°)$ at room temperature (~295 K) and has been discussed in detail in several earlier reports.[1–6,16–19] It will be noted that the line shape evolves steadily from a singlet to a doublet, almost as if the mixed-lattice spectra were a result of a simple superposition of those from the individual components. In order to check this possibility the spectra were reexamined by comparing them with those obtained by their algebraic addition. Figure 2 shows the results for $x=0.5$. For convenience of comparison, the spectra for pure ADP and RDP are reproduced in Figs. 2(a) and 2(b), respectively, and their algebraic sum (simple addition) is shown in Fig. 2(c). The spectrum of Fig. 2(c) was found to be identical with that obtained from the crystals of RDP and ADP glued together [Fig. 2(d)]. In general, the spectra observed from the RADP crystals were found to be different, as may be noted from Fig. 2(e) which shows a typical, experimentally observed spectrum for $x=0.5$. It is noted that the mixed lattice shows a spectrum which is significantly shifted toward the center, as compared to Figs. 2(c) or 2(d), implying that the probe responds to the mixed lattice fairly characteristically. Thus the spectrum of a mixed crystal is not just an algebraic sum of the spectra of pure ADP and pure RDP. Nevertheless, it seemed clear that the spectrum of Fig. 2(e) still could be analyzed as being composed of the signals of the pure compounds by assuming that the mixing process causes changes in both the positions and widths of the signals. This hypothesis was tested by application of a fitting procedure. To simplify the mathematical procedure, the integrated spectra were used. The experimental spectra of the mixed crystals were fitted from a com-

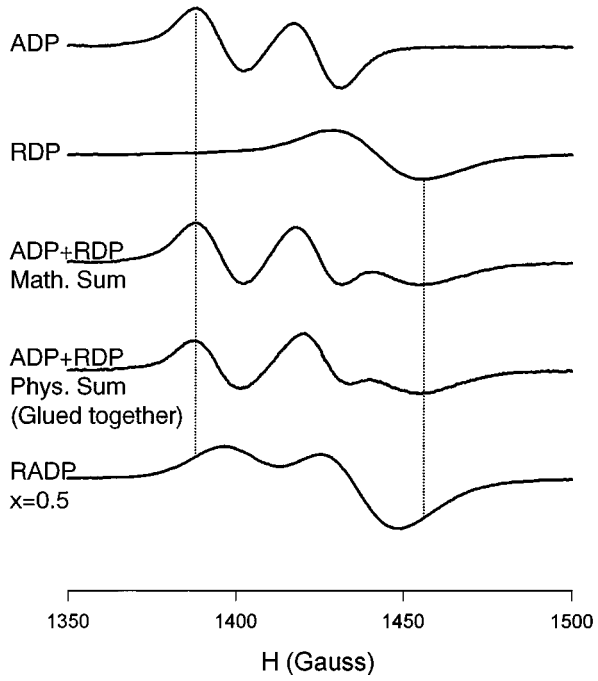

FIG. 2. EPR spectra of the RADP system: pure ADP (a), pure RDP (b), the mathematical sum of the spectra (c), the spectrum of an RDP and an ADP crystal glued together (d), and of an RADP mixed crystal with $x=0.5$ (e).

bination of the ADP signal (Gaussian line shape in the integrated spectrum) and the RDP signal (double Gaussian line shape). The fitting parameters were the amplitudes, linewidths, and the positions of both the Gaussian and the double Gaussian signal. Satisfactory results were obtained for every composition. An example ($x=0.5$) is shown in Fig. 3. As may be noted, a plot of the area under the signal from either of the components versus the system composition x yields a straight line with unity slope, showing that indeed the theoretically obtained amplitudes of the postulated component signals match the actual composition of the mixed crystals closely (Fig. 4). The straightforward conclusion is that the experimental EPR signal of RADP is indeed composed of two distinct components, representing a local anti-

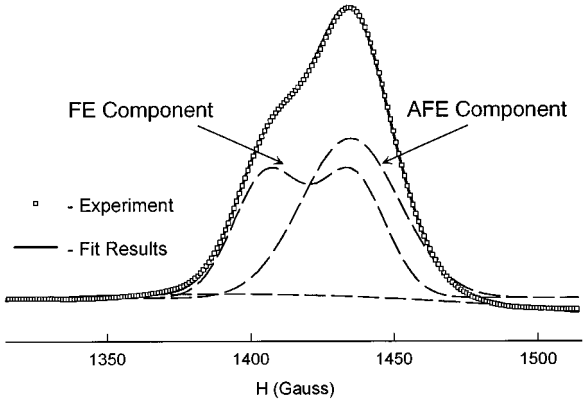

FIG. 3. Comparison of experimental and theoretical spectra for an RADP mixed crystal ($x=0.5$); rectangles: experimental signal; full line: theoretical signal obtained by fitting; dashed lines: the two components of the theoretical signal.

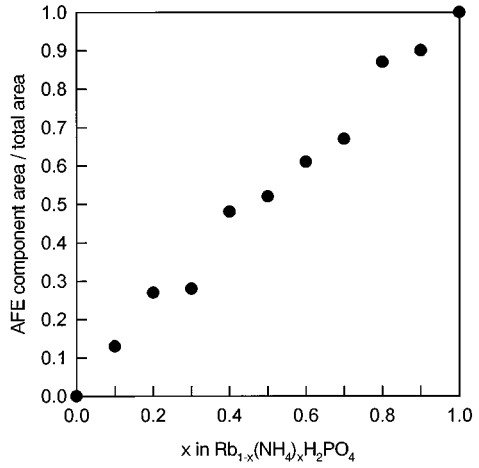

FIG. 4. Plot of the component signal integrals (as obtained by the fitting procedure) versus the mixed crystal composition.

ferroelectric and ferroelectric state of the AsO_4^{4-} unit as seen in the pure RDP and ADP spectra. These observations formed the basis of our theoretical model as discussed in the next section.

V. THEORETICAL MODEL

In order to further interpret the parameters of the compound signals as obtained by the fitting procedure, and to explain their linewidths and positions, a statistical approach was used. Assuming that a neighboring Rb^+ ion has a tendency to impose a ferroelectric orientation on the AsO_4^{4-} units, and an NH_4^+ group has the opposite effect, the probability of the observed unit being in each of the two possible states can be determined from the number of influencing neighbors and the composition of the system. In a first-order approximation, it was assumed that around the AsO_4^{4-} probe there are a total of n cations that can influence the spectrum. The probability that m of the n significant neighbors are NH_4^+ ions can be expressed as

$$p_m(n,x)=\frac{n!x^m(1-x)^{n-m}}{(n-m)!m!}, \tag{1}$$

where x is the fraction of ADP in the mixed lattice ($0\leqslant x\leqslant 1$).

The assumption that Rb^+ and NH_4^+ neighbors influence the ^{75}As hyperfine coupling for an AsO_4^{4-} center with equal strength leads to the following expression for an $H_2AsO_4^{4-}$ unit to be in the antiferroelectric configuration:

$$p_{\mathrm{AFE}}(n)=\frac{m}{n}. \tag{2}$$

Combining (1) and (2) gives the probability to find an antiferroelectrically oriented unit with m NH_4^+ neighbors around

$$P_{\mathrm{AFE},m}(n,x)=p_m(n,x)\left(\frac{m}{n}\right). \tag{3}$$

Using the linear dependence of the ^{75}As hyperfine splitting on the system composition,[2] the line position $H_m(n)$ of the component of the signal can be expressed as

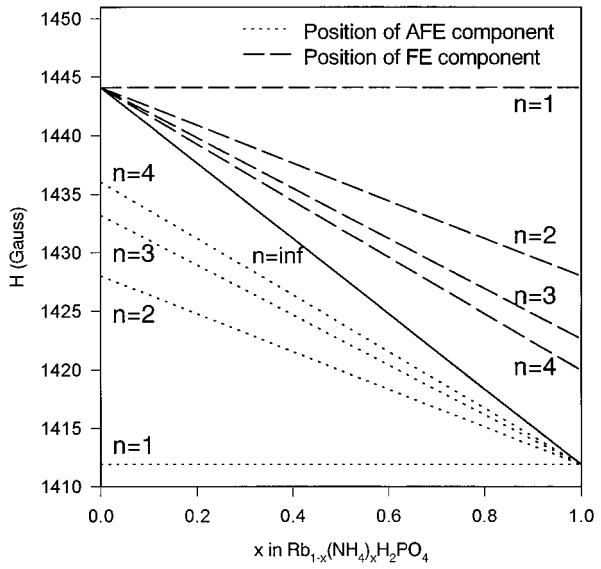

FIG. 5. Plot of H_{FE} and H_{AFE} versus the system composition x. The different lines reflect the different values for n.

$$H_m(n)=H_{\mathrm{AFE}}\frac{m}{n}+H_{\mathrm{FE}}\frac{n-m}{n}, \tag{4}$$

where H_{FE} and H_{AFE} are the line positions of pure RDP (FE) and ADP (AFE). The line position of the total antiferroelectric component of the signal of a given RADP system can then be obtained by calculating the average over the line positions of all the AsO_4^{4-} units, weighted by the probabilities of their occurrence,

$$\overline{H_{\mathrm{AFE}}}(n,x)=\frac{\Sigma_{m=0}^{m=n}p_{\mathrm{FE},m}(n,x)H_m(n)}{\Sigma_{m=0}^{m=n}p_{\mathrm{AFE},m}(n,x)}, \tag{5}$$

where the denominator serves as a normalization constant. Substitution of (1), (3), and (4) in (5) and subsequent simplification (see Appendix) yields

$$\overline{H_{\mathrm{AFE}}}(n,x)=H_{\mathrm{FE}}+(H_{\mathrm{AFE}}-H_{\mathrm{FE}})\frac{1+(n-1)x}{n} \tag{6}$$

as the function describing the line position of the overall ferroelectric contribution to the EPR signal and its dependence on x and n. An analogous expression can be obtained for $\overline{H_{\mathrm{FE}}}(n,x)$:

$$\overline{H_{\mathrm{FE}}}(n,x)=H_{\mathrm{AFE}}+(H_{\mathrm{FE}}-H_{\mathrm{AFE}})\frac{1+(n-1)(1-x)}{n}. \tag{7}$$

As can be seen, for any given n the line positions are linearly dependent on x.

Figure 5 shows a plot of this dependence for different values of n. For $n=\infty$, one obtains a straight line between the line positions H_{FE} and H_{AFE} of the pure compounds. For all other values of n, there is a pair of corresponding lines for the FE and AFE contributions. The lines of each pair have equal slopes, with a vertical distance Δ_n between them. This distance corresponds to the difference $\overline{H_{\mathrm{FE}}}(n,x)-\overline{H_{\mathrm{AFE}}}(n,x)$, and subtraction of (6) from (7) can be used to derive the relationship

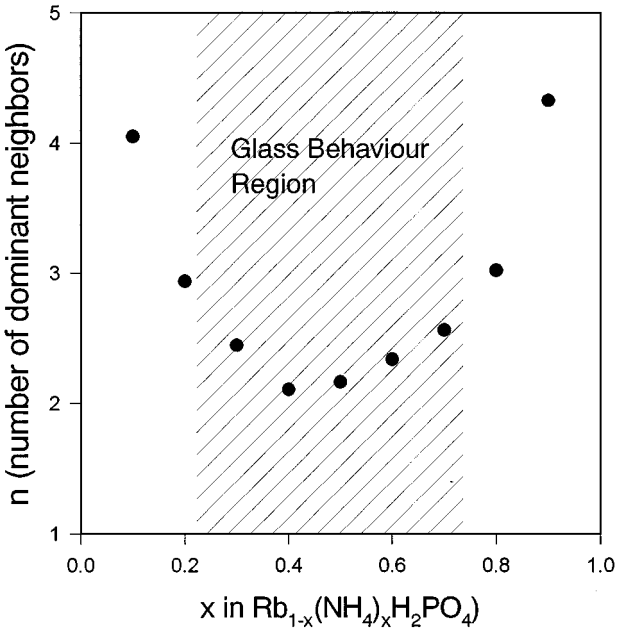

FIG. 6. Plot of the interaction range parameter n vs the system composition x; the hatched area corresponds to the range of x where an FE/AFE ordered phase does not exist (Refs. 7, 8, and 10).

$$n=\frac{H_{\mathrm{FE}}-H_{\mathrm{AFE}}}{\overline{H_{\mathrm{FE}}}-\overline{H_{\mathrm{AFE}}}}=\frac{\Delta}{\Delta_n}, \tag{8}$$

where Δ is the difference in the line positions for the spectra of pure RDP and ADP, i.e., $\Delta=H_{\mathrm{FE}}-H_{\mathrm{AFE}}$. If experimental values for Δ and Δ_n could be obtained, this equation would allow the determination of the parameter n.

Experimentally, Δ can be obtained easily by recording the spectra of pure RDP and ADP. Δ_n, on the other hand, is the difference in the line positions for the FE and AFE contributions to the observed signal from the mixed crystal as obtained from the fitting procedure described above. In Fig. 6 the results for n obtained from our EPR spectra are depicted. The plot shows that the range of interactions (represented by n) is biggest in the vicinity of $x=0$ and $x=1$, whereas for $x\approx 0.4$, n reaches its minimum. Another very significant observation was the asymmetry of the plot in Fig. 6. The same dielectric studies which reported[7,8,10] that the range of x where no ferroelectric or antiferroelectric low-temperature phase exists is $0.21<x<0.74$, also showed that the formation of an ordered phase is a little more favored on the NH_4-rich side of the diagram than on the Rb-rich side. This is in full accordance with our result that the range of interactions seems to be slightly smaller on the Rb-rich side. It also appears as if there is a threshold value for the parameter n ($n\approx 2.8$), below which an ordered phase cannot exist.

Another interesting result which can be obtained from Fig. 6 is the fact that at the minimum of the experimental curve, the parameter n approaches 2. Since one of the main assumptions in our model is that n signifies neighbors of equal influence on the group, and there are two closest neighbors for every PO_4/AsO_4 group in the unit cell, it seems safe to assume that at least for system compositions around $x=0.5$, the range of interactions in the crystal is limited to one unit cell. For other values of x, the interaction range

seems to increase. This result is in line with the notion that short range cationic interactions are the signatures of the formation of the RADP glass.

VI. CONCLUSION

In the present study, we were able to show that in the EPR spectra of RADP crystals the spectra from the two possible (ferroelectric/antiferroelectric) states of the $(P, As)O_4$ tetrahedra can be clearly distinguished for all values of system composition x. Using only very general assumptions, we were able to derive a relationship between the relative shift of the component signal and an interaction range parameter n, representing a (hypothetical) shell of neighbors with equal influence on the central tetrahedron. Thus experimental values for this parameter were obtained from the observed spectra. For system compositions around $x=0.5$, n corresponds to the number of closest neighbors the tetrahedron has in the unit cell, indicating that the range of interactions in mixed crystals of these compositions is limited to the unit cell. For other compositions, the range of interactions is significantly larger. It is worth emphasizing that all the measurements were made at ambient temperatures, but we could still obtain valuable information related to the RADP composition range which shows glassy behavior.

As alluded to in the Introduction, two contrasting interpretations of essentially the same spectra have been reported. The first one[2] proposed that the spectral changes can only be explained in terms of the effects of a fast ($\tau=10^{-8}$ s) exchange between adjacent ferroelectric and antiferroelectric configurations. In contrast, a subsequent study[5] ascribed the line shape changes to just spectral overlap and broadening due to lattice strain (caused by structural and bonding mismatch), without presenting any mechanistic details. The results obtained in the present work disagree with the ''fast ferroelectric-antiferroelectric exchange'' model because for every composition we have two hyperfine parameters, rather than only one (as expected from the fast exchange model[2]). On the basis of a fairly satisfactory agreement between the experimentally observed and (presently) simulated spectra (as may be noted from Fig. 2, for example) we conclude that the observed spectra can be well understood in terms of the presently suggested statistical model, without any contribution from motional effects.

In summary, for the RADP system these results provide information that is relevant to the range of interactions. It thus appears that this procedure provides an easy and quick methodology for assessing the composition over which one might expect glassy behavior. With a broader view, and since the analysis procedure used is fairly general, the methodology should in principle be applicable to a wide range of systems with competing interactions. As long as the individual contributions can be spectroscopically separated for a given composition, it should be possible to utilize these parameters for assessing the range of interactions in the system for that composition. Thus the same methodology might be applicable to ^{31}P or ^{75}As NMR studies of phosphate- and arsenate-based proton glasses and related mixed systems.

ACKNOWLEDGMENTS

We gratefully acknowledge the U.S. Department of Energy and the U.S. Bureau of Mines for partial support of this research.

APPENDIX

In order to obtain Eq. (6) from Eq. (5) it is useful to derive three intermediate equations [(A1)–(A3)]

$$\sum_{m=0}^{n} \frac{n!x^m(1-x)^{n-m}}{(n-m)!m!} = \sum_{m=0}^{n} C_m^n x^m (1-x)^{n-m} = [x+(1-x)]^n = 1. \tag{A1}$$

This directly follows from binomial expansion $(a+b)^n=\sum_{m=0}^{n} C_m^n a^m b^{n-m}$,

$$\sum_{m=0}^{n} \frac{n!x^m(1-x)^{n-m}m}{(n-m)!m!n} = x\sum_{m=1}^{n} \frac{n!x^{m-1}(1-x)^{n-m}m}{(n-m)!m!n} = x\sum_{i=0}^{k} \frac{k!x^i(1-x)^{k-i}}{(k-i)!i!}, \text{ where } k=n-1 \text{ and } i=m-1$$
$$= x, \quad \text{using Eq (A1).} \tag{A2}$$

And, finally

$$\sum_{m=0}^{n} \frac{n!x^m(1-x)^{n-m}m^2}{(n-m)!m!n^2} = x\sum_{i=0}^{k} \frac{k!x^i(1-x)^{k-i}(i+1)}{(k-i)!i!(k+1)}, \quad \text{where } k=n-1 \text{ and } i=m-1$$
$$= \frac{x}{k+1}\left(\sum_{i=0}^{k} \frac{k!x^i(1-x)^{k-i}i}{(k-i)!i!}+1\right) = \frac{x}{k+1}(kx+1), \quad \text{using Eq. (A2)}$$
$$= \frac{x}{n}(nx-x+1), \quad \text{on substituting back } n=k+1. \tag{A3}$$

Now we can simplify Eq. (5) by substituting Eqs. (3) and (4):

$$\overline{H_{\mathrm{AFE}}}(n,x)=\frac{\Sigma_{m=0}^{m=n}\dfrac{n!x^m(1-x)^{n-m}}{(n-m)!m!}\dfrac{m}{n}\left(H_{\mathrm{AFE}}\dfrac{m}{n}+H_{\mathrm{FE}}\dfrac{n-m}{n}\right)}{\Sigma_{m=0}^{m=n}\dfrac{n!x^m(1-x)^{n-m}}{(n-m)!m!}\dfrac{m}{n}}. \tag{A4}$$

Then, using Eqs. (A1), (A2), and (A3), Eq. (A4) becomes

$$\overline{H_{\mathrm{AFE}}}(n,x)=H_{\mathrm{FE}}+(H_{\mathrm{AFE}}-H_{\mathrm{FE}})\,\frac{1+x(n-1)}{n}.$$

*Current address: Department of Chemistry, Florida State University, Tallahassee, Florida 32306-3006.

[1] S. Waplak, Z. Trybula, J. E. Drumheller, and V. H. Schmidt, Phys. Rev. B **42**, 7777 (1990).
[2] Y. Babu, M. D. Sastry, and B. A. Dasannacharya, J. Phys. Condens. Matter **4**, 1819 (1992).
[3] P. K. Kahol and N. S. Dalal, Ferroelectrics **156**, 303 (1994).
[4] R. Xu, P. K. Kahol, and N. S. Dalal, Ferroelectrics **156**, 377 (1994).
[5] P. K. Kahol, D. T. Scoular, and N. S. Dalal, J. Phys. Condens. Matter **6**, 2971 (1994).
[6] Y. Babu, M. D. Sastry, and B. A. Dasannacharya, J. Phys. Condens. Matter **6**, 2975 (1994).
[7] E. Courtens, J. Phys. Lett. **43**, L199 (1982).
[8] E. Courtens, Ferroelectrics **72**, 157 (1987).
[9] V. H. Schmidt, Ferroelectrics **72**, 157 (1987).
[10] E. Courtens, in *Dynamics of Molecular Crystals*, edited by J. Lascombe (Elsevier, Amsterdam, 1987), pp. 301–315.
[11] J. Slak, R. Kind, R. Blinc, E. Courtens, and S. Zumer, Phys. Rev. B **30**, 80 (1984).
[12] R. Blinc, J. Dolinsek, V. H. Schmidt, and D. C. Alion, Europhys. Lett. **6**, 55 (1988).
[13] A. Levstik, C. Filipic, Z. Kutnjak, I. Levstik, R. Pirc, B. Tadic, and R. Blinc, Phys. Rev. Lett. **66**, 2368 (1991).
[14] E. Matsushita and T. Matsubara, Prog. Theor. Phys. **71**, 235 (1984).
[15] See, for example, M. E. Lines and A. M. Glass, *Principles and Applications of Ferroelectrics and Related Materials* (Clarendon, Oxford, 1977), Chap. 9.
[16] N. S. Dalal, Ad. Magn. Reson. **10**, 119 (1982).
[17] N. S. Dalal, J. P. DeLooze, and R. Blinc (unpublished).
[18] N. S. Dalal, J. R. Dickinson, and C. A. McDowell, J. Chem. Phys. **57**, 4254 (1972).
[19] N. S. Dalal, J. A. Hebden, D. E. Kennedy, and C. A. McDowell, J. Chem. Phys. **66**, 4425 (1977).
[20] S. Hayase, K. Kamon, H. Sakashita, and H. Terauchi, J. Phys. Soc. Jpn. **55**, 2695 (1986).
[21] N. S. Dalal, C. A. McDowell, and R. Srinivasan, Mol. Phys. **24**, 417 (1972).
[22] P. Cevc and M. Schara, Phys. Status Solidi A **30**, 357 (1975).